ISSN 0016-7029, Geochemistry International, 2007, Vol. 45, No. 9, pp. 882–899. © Pleiades Publishing, Ltd., 2007.
Original Russian Text © I.A. Tararin, Z.G. Badredinov, S.I. Dril', 2007, published in Geokhimiya, 2007, No. 9, pp. 962–980.

Geochemistry and Age of Metamorphic Rocks of the Khavyven Highland, Eastern Kamchatka

I. A. Tararin[a], Z. G. Badredinov[a], and S. I. Dril'[b]

[a] *Far East Geological Institute, Far East Division, Russian Academy of Sciences, pr. Stoletiya Vladivostoka 159, Vladivostok, 690022 Russia*
e-mail: itararin@mail.ru

[b] *Vinogradov Institute of Geochemistry, Siberian Division, Russian Academy of Sciences, ul. Favorskogo 1a, Irkutsk, 664033 Russia*
e-mail: sdril@igc.irk.ru

Received October 28, 2005

Abstract—The metamorphic rocks of the Khavyven Highland in eastern Kamchatka were determined to comprise two complexes of metavolcanic rocks that have different ages and are associated with subordinate amounts of metasediments. The complex composing the lower part of the visible vertical section of the highland is dominated by leucocratic amphibole–mica (±garnet) and epidote–mica (±garnet) crystalline schists, whose protoliths were andesites and dacites and their high-K varieties of the island-arc calc–alkaline series. The other complex, composing the upper part of the vertical section, consists of spilitized basaltoids transformed into epidote–amphibole and phengite–epidote–amphibole green schists, which form (together with quartzites, serpentinized peridotites, serpentinites, and gabbroids) a sea-margin ophiolitic association. The high LILE concentrations, high K/La, Ba/Th, Th/Ta, and La/Nb ratios, deep Ta–Nb minima, and low $(La/Yb)_N$ and high $^{87}Sr/^{86}Sr$ ratios of the crystalline schists of the lower unit are demonstrated to testify to their subduction nature and suggest that their protolithic volcanics were produced in the suprasubduction environment of the Ozernoi–Valaginskii (Achaivayam–Valaginskii) island volcanic arc of Campanian–Paleogene age. The green schists of the upper unit show features of depleted MOR tholeiitic melts and subduction melts, which cause the deep Ta–Nb minima, and low K/La and $^{87}Sr/^{86}Sr$ ratios suggesting that the green schists were formed in a marginal basin in front of the Ozernoi–Valaginskaya island arc. Recently obtained K–Ar ages in the Khavyven Highland vary from 32.4 to 39.3 Ma and indicate that the metamorphism of the protolithic rocks occurred in the Eocene under the effect of collision and accretion processes of the arc complexes of the Ozernoi–Valaginskii and Kronotskii island arcs with the Asian continent and the closure of forearc oceanic basins in front of them. The modern position of the collision suture that marks the fossil subduction zone of the Ozernoi–Valaginskii arc and is spatially restricted to the buried Khavyven uplift in the Central Kamchatka Depression, which is characterized by well-pronounced linear gravity anomalies.

DOI: 10.1134/S0016702907090030

INTRODUCTION

The island structures of Kamchatka (Fig. 1) are currently thought to have been formed in the Late Meso-Cenozoic under the effect of accretion–collision processes [1–12 and others]. One of the principal events in the geological history of the area was the collision of the Achaivaam–Valaginskii [4] or Ozernoi–Valaginskii [1, 5] island arc and the continent, when the Cretaceous deposits of the marginal sea and island arc were thrust over the heterogeneous material of the Asian continental margin.

According to the predominant composition of the stratified Upper Cretaceous complexes, the Olyutorskii–Kamchatka territory is subdivided into northwestern (western Kamchatka–Ukelayat) and southeastern (eastern Kamchatka–Olyutorskii) zones [13, 14]. The Upper Cretaceous of the northwestern zone is dominated by deep-sea sand–shale complexes, which were formed near the foot of the continental slope of passive margins [15]. The composition of the sedimentary rocks suggests that their eroded source areas were dominated by extensively tectonized volcanic–sedimentary sequences, and the erosion level was not deep. The Late Cretaceous sequences of the southeastern zone consist mostly of volcanic rocks (mostly tuffs and tuff–sedimentary rocks), which compose inliers in Cenozoic deposits [10]. The largest exposures of the Upper Cretaceous volcanic rocks occur in the Olyutorskii and Vetveiskii ranges of the Koryak Highland, in the northern and southern parts of the Sredinnyi Range, and in eastern Kamchatka ranges. They are accompanied by tectonic lenses of serpentinites and gabbroids, which are thought to be fragments of ophiolitic complexes.

The boundary between the Late Cretaceous volcanic rocks of the southeastern zone and the coeval terrigenous complexes of the northwestern zone is the large

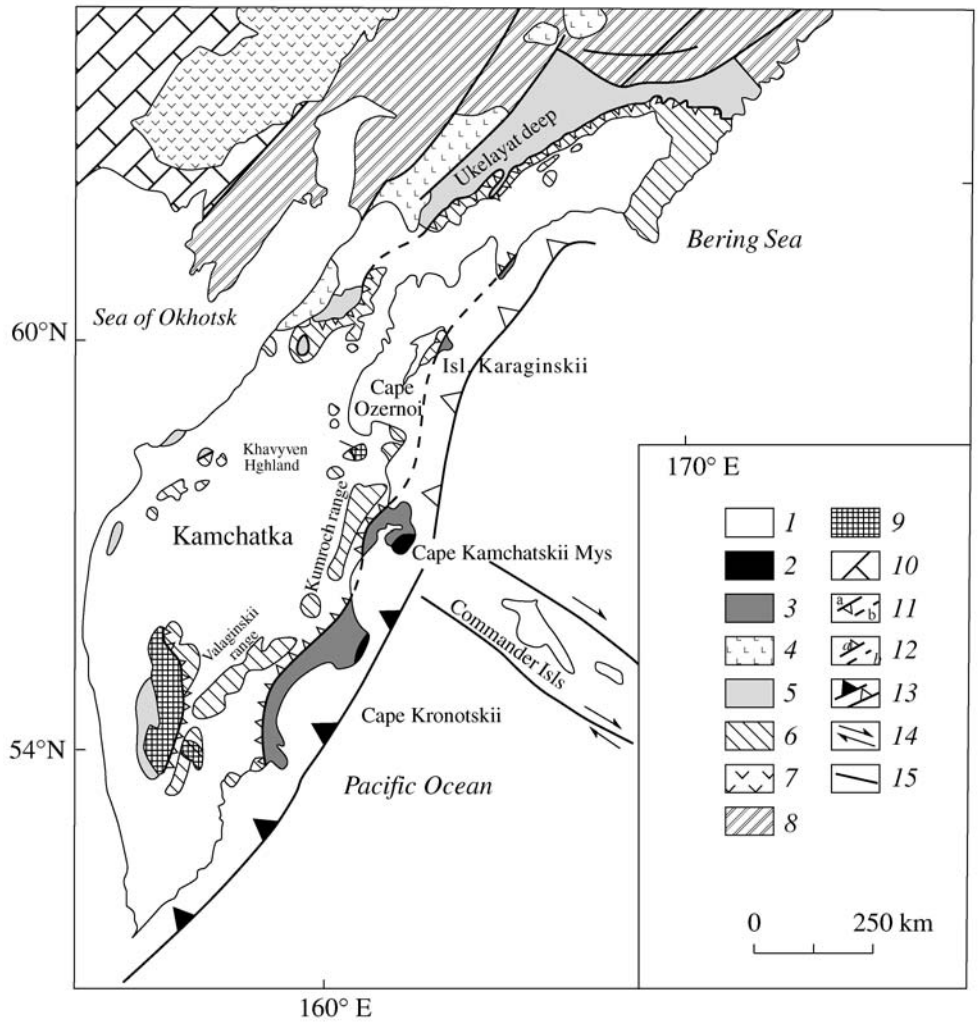

Fig. 1. Schematic tectonic map of Kamchatka and the Koryak Highland (after [5]).
(*1*) Cenozoic cover; (*2*) Kronotskii fossil island arc (Late Cretaceous–Eocene); (*3*) eastern Kamchatka accretionary zone; (*4*) western Kamchatka–Koryak volcanic belt (Middle Eocene–Oligocene); (*5*) Ukelayat–Lesnovskii deep (Late Cretaceous–Middle Eocene); (*6*) Ozernoi–Valagninskii (Achaivayam–Valaginskii) fossil island arc (Late Cretaceous–Paleocene); (*7*) Okhotsk–Chukot volcanic belt (Early–Late Cretaceous); (*8*) accreted Mesozoic terranes; (*9*) metamorphic complexes of the Sredinnyi and Ganal'skii ranges and the Khavyven Highland; (*10*) pre-Cretaceous complexes of Siberia; (*11*) Vatyn–Lesnovskii–Andrianovskii suture: (a) observed, (b) inferred; (*12*) Tyushevskii–Govenskii suture–Grechishkin overthrust: (a) observed, (b) inferred; (*13*) subduction zones: (a) modern, (b) fossil; (*14*) strike–slip faulting zones; (*15*) faults.

Vatyn–Lesnovskii–Andrianovskii suture, which developed in the Eocene–Early Miocene and is overlain by Middle Eocene volcanic rocks of the Kinkil'skaya Formation and intruded by granitoids comagmatic with them [4, 5, 10, 16, 17].

The Khavyven Highland in the western part of Ozernoi Peninsula in eastern Kamchatka is restricted to the southeastern zone of Upper Cretaceous volcanic complexes in the northern part of the Central Kamchatka Trough. The latter is filled with Quaternary loose terrigenous and volcanic rocks. Geological survey and specialized geological research in the area made it possible to thoroughly study the geology of the highland and to obtain data on the composition and mineralogy of its low-temperature metamorphic rocks [18–20]. At the same time, the geochemistry of the rocks and the age of their metamorphic transformations remain uncertain. Because of this, our research was centered on obtaining instrumental geochemical data to assay the geodynamic environment in which the protolithic rocks of the Khavyven Highland were produced.

METHODS

Minerals were analyzed on a Camebax microprobe at the Institute of Volcanology and Seismology, Far East Division, Russian Academy of Sciences, Petropavlovsk-Kamchatskii, at an accelerating voltage of 20 kV and a current of 50 mA, accurate to no worse than 3%.

Major elements were determined by conventional "wet" chemical techniques at the Far East Geological Institute, Far East Division, Russian Academy of Sciences, Vladivostok.

Trace elements (including REE) were determined by ICP-MS at the Irkutsk Analytical Center for Collective Use on a VG Plasmaquad PQ2+ mass spectrometer. The device was calibrated on the BHVO-1, AVG-1, and BIR-1 internationally certified standards and the U-94-5 in-laboratory basanite standard. The (1 σ) standard deviation during replicate analyses for most elements did not exceed 5% and was no higher than 10% for Pr (Ce and Ta in AVG-1). The precision of Pb measurements in BHVO-1 was 5–10%. The Ni concentrations were determined by quantitative spectral techniques at the Far East Geological Institute, Far East Division, Russian Academy of Sciences.

The Sr isotopic composition was determined at the Vinogradov Institute of Geochemistry, Siberian Division, Russian Academy of Sciences, on a MI-1201T mass spectrometer in single-beam mode. Samples were prepared for mass spectrometric analysis following the conventional methods described in [21]. The accuracy of the isotopic analyses was monitored by replicate analyses of the VNIIM standard, whose $^{87}Sr/^{86}Sr$ ratio was equal to 0.70800 ± 13 (n = 26) at a recommended value $^{87}Sr/^{86}Sr$ = 0.708028 [22]. The $^{87}Sr/^{86}Sr$ isotopic ratios measured in the samples were not normalized to the recommended value for the VNIIM standard.

GEOLOGY OF THE METAMORPHIC ROCKS

The metamorphic rocks of the Khavyven Highland are exposed in the northern part of the large Khavyven uplift of the basement structures of the Central Kamchatka Trough, which was traced for ~500 km, from the latitude of the settlement of Mil'kovo in the south to Uala Bay in the north, using gravimetric and magnetometric data [23, 24]. The uplift is characterized by a broad zone of positive linear gravity anomalies bounded by steep gradient steps, which represent large faults. Within the highland itself, the gravity field shows the maximum values, and other blocks of the Khavyven uplift are overlain by Paleogene–Neogene deposits. It is, however, thought that their basement is compositionally similar to the rocks of the Khavyven uplift [25]. The Khavyven uplift can be regarded as a "fossil Benioff zone, from which an obduction nappe of volcanic–siliceous deposits was thrust eastward" [24, p.69].

The Khavyven Highland is composed of rocks metamorphosed to the greenschist facies that are now combined into the Khavyven Formation, with the age of its protolith remaining uncertain. The metamorphic rocks of the formation compose most of the Khavyven Highland and occupy an area of approximately 150 km^2 (Fig. 2). Late Cretaceous (Santonian–Campanian) coarse-fragment volcanic rocks of the Khapitskaya Formation (coeval with the Iruneiskaya Formation in Central Kamchatka, Valaginskii Formation in the Valaginskii Range, and the Vatynskii Formation in the Koryak Highland) are exposed in the western slopes of the highland. These rocks are separated from the metamorphic rocks by a subvertical fault. The basaltoids of these formations display geochemical features of both oceanic volcanics (mostly MORB) and arc rocks [1, 26, 27]. In the south, the metamorphic rocks of the Khavyven Formation are unconformably overlain by Miocene terrigenous–volcanic deposits [18–20].

The Khavyven Formation is subdivided into two members: (1) a lower member of leucocratic amphibole–mica (±garnet) and epidote–mica (±garnet) thinly banded crystalline schists and micaceous (±garnet) quartzite-schists with an apparent thickness of about 500 m and (2) an upper member of epidote–amphibole and phengite–amphibole green schists and epidote–amphibole–mica quartzites with an overall thickness of approximately 750 m. The lower unit is exposed in the core of a dome-shaped structure trending to the northwest in the eastern and southeastern parts of the Khavyven Highland (Fig. 2). The boundary between the units was observed in the valley of the Pravaya Kvartsevaya River and is drawn along the boundary between the layers of mica and garnet–mica quartzite-schists of the lower unit and the melanocratic epidote–amphibole green schists of the upper unit.

The most complete succession of the lower unit is exposed in the second left-hand tributary of the Pravaya Kvartsevaya River (Fig. 2, sites 1184–1187). The bottom of the visible part of the vertical section is composed there of garnet–epidote–amphibole–mica, epidote–amphibole–mica, and epidote–mica leucocratic crystalline schists with beds of chlorite–epidote–amphibole and garnet–amphibole–mica green schists. These rocks are overlain by intercalating biotite–amphibole and epidote–amphibole–mica (often with garnet) thinly banded crystalline schists. The upper part of the unit is dominated by leucocratic thinly banded amphibole–mica, garnet–amphibole–mica, and epidote–mica crystalline schists intercalating with beds of mica (±garnet, ±amphibole, ±epidote) quartzites and quartzite-schists.

The upper unit is exposed in most of the Khavyven Highland and is spatially restricted to the limbs of a dome-shaped structure, whose core consists of the rocks of the lower unit (Fig. 2). According to the lithology of its rocks, the upper unit can be subdivided into two members: lower (green schists) and upper (quartzites). The member of green schists has a thickness of approximately 450 m and consists of intercalating banded epidote–amphibole (predominant) and phengite–epidote–amphibole and chlorite–epidote–amphibole green schists with subordinate amounts of banded two-mica (±garnet, ±epidote, ±amphibole) quartzite beds, whose amount gradually increases toward the upper portions of this member. The apparent thickness of the upper quartzites is about 150 m.

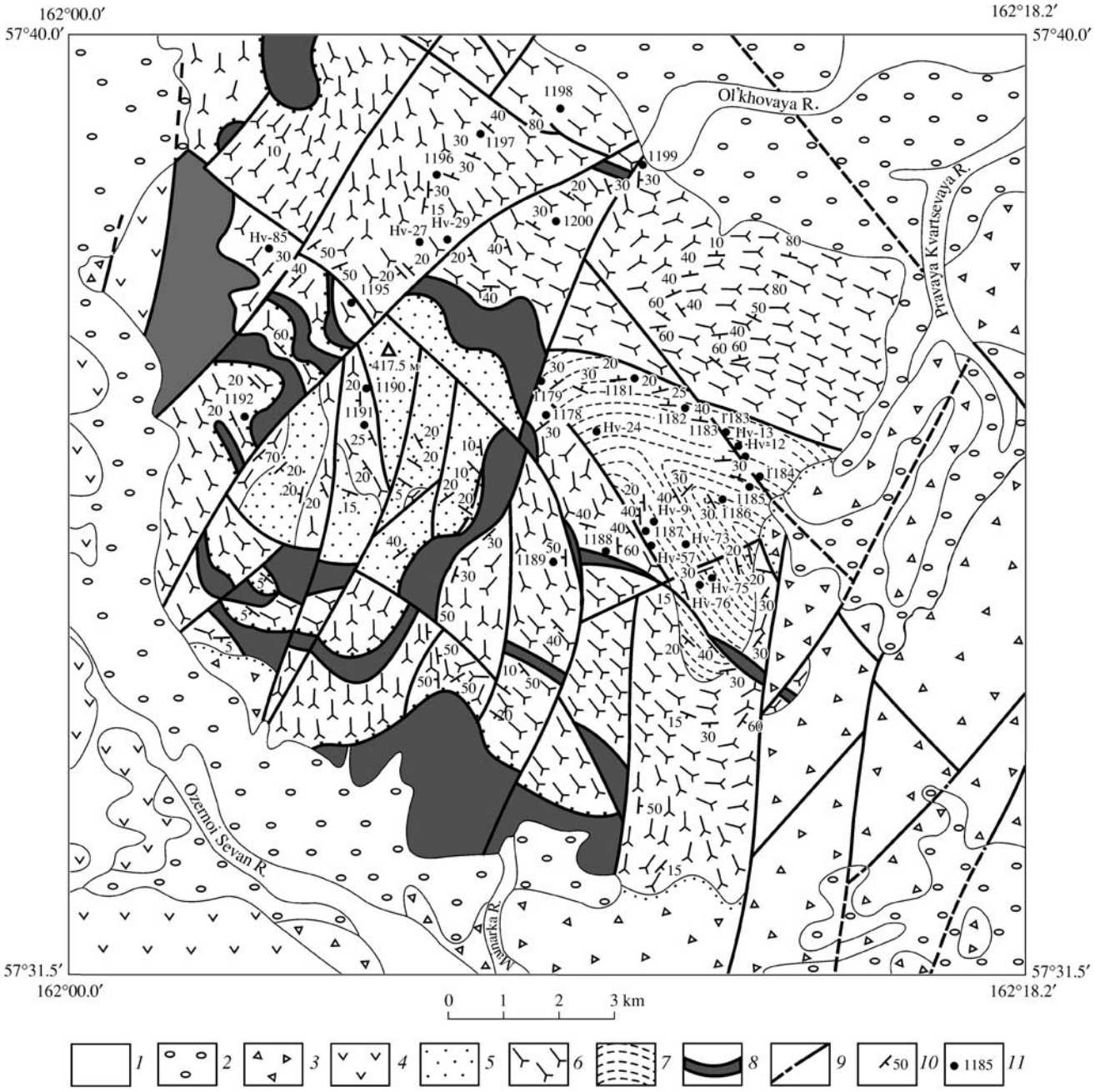

Fig. 2. Schematic geological map of the Khavyven Highland (modified after [19, 20]).
(*1*) Modern alluvial deposits; (*2*) modern lacustrine–limnic, glacial, diluvial, and alluvial deposits; (*3*) Cenozoic terrigenous–volcanic deposits; (*4*) Late Cretaceous (Campanian) volcanic rocks (Khapitskaya Formation); (*5*–*7*) Khavyven Formation: (*5*, *6*) upper unit: (*5*) upper quartzite subunit, (b) lower green schist subunit, (*7*) lower unit: metavolcanic leucocratic amphibole–mica (±garnet) and epidote–mica (±garnet) crystalline schists; (*8*) apoharzburgite serpentinite and serpentinite; (*9*) faults; (*10*) strike and dip symbols of schistosity, layering, and lineation; (*11*) sampling and observation sites, mentioned in the text.

The whole vertical section of the upper unit includes bodies of serpentinites, serpentinized harzburgites, dunites, and accompanying gabbroids, whose thickness varies from a few to 60–100 m (Fig. 2). The thickest peridotite bodies occur near the boundary between the members of green schists and quartzites. The close spatial association of the metavolcanics and quartzites, serpentinites, serpentinized harzburgites, and gabbroids in the upper unit of the Khavyven Formation suggest that they compose a metamorphosed ophiolite complex [18–20, 28, 29].

PETROLOGY AND MINERALOGY OF THE METAMORPHIC ROCKS

The *crystalline schists of the lower unit* are porphyroblastic rocks consisting of garnet, amphibole, and biotite porphyroblasts up to 1–2 mm across and larger (up to 2–3 mm) tabular crystals of albite and, more rarely, potassic feldspar in a fine-grained groundmass consisting of various proportions of albite, quartz, potassic feldspar, biotite, muscovite–phengite, epidote, and amphibole. The blastoporphyritic texture of the crystalline schists reflects the porphyritic texture of their protolithic volcanics.

The composition of minerals from the major varieties of the crystalline schists is reported in Table 1. [1] As can be seen from this table, the plagioclase of the rocks is nearly pure albite, and their potassic feldspar contains no more than 3–5% of the albite end member. As other mafic minerals, the garnets are highly ferrous and display prograde zoning of their crystals, which indicates that the minerals crystallized at an increasing temperature during prograde metamorphism. The prograde type of the zoning of garnet grains is in conflict with the earlier idea [30] about the diaphthoric nature of rocks composing the Khavyven Highland as produced by the low-temperature transformations of precursor gneisses.

Amphiboles in the crystalline schists have a greenish blue to bluish green color and compositionally correspond to calcic amphibole: actinolite, ferroactinolite, magnesian, and ferrous hornblende (according to the systematics [31]). The marginal zones of the crystals have a more intense bluish color because of younger zones of Ca–Na amphibole like winchite and barroisite.

The *quartzites and quartzite–schists* of the lower unit are banded rocks consisting of quartz (40–60 vol %), albite (up to 20–25%), and mafic minerals, predominantly epidote, muscovite–phengite, chlorite, and biotite, with amphibole and garnet contained in strongly subordinate amounts. The garnet-bearing quartzite–schists and quartzites contain barroisite, a Ca–Na amphibole (Table 1, sample 1182).

The *green schists of the upper unit* are dominated by albite, bluish green amphibole, and variable proportions of epidote, chlorite, muscovite–phengite, and ore minerals. Amphibole accounts for 30–50% of the rocks by volume, epidote for 10–40%, and albite for 20–40%. The rocks also usually contain no more than 5–10% chlorite, muscovite–phengite, and ore minerals. The accessory minerals are apatite, sphene, magnetite, titanomagnetite, and, more rarely, ilmenite. The green schists are rich in sulfides, predominantly pyrite. Amphibole and albite compose the groundmass of the rocks and porphyroblasts up to 1–3 mm in size, which reflect the relict porphyritic texture of the protolithic volcanics.

Many features of minerals mentioned in the description of the crystalline schists are also typical of the rocks composing the upper unit. For example, the plagioclase of the green schists and quartzites is rich in albite and contains no more than 1% of the anorthite end member. Analogous compositions and zoning are also characteristic of amphiboles of actinolite, winchite, and barroisite composition (Table 2). The margins of amphibole crystals typically show a transition from calcic amphibole in the core to calcic–sodic amphibole in the margins. All amphiboles of the green schists, particularly the actinolite and barroisite in the magnetite–albite–barroisite–epidote–garnet rocks, are enriched in Mn (up to 7 wt % MnO) [19], and their concentrations of major and trace elements are close to those in the Fe–Mn crusts of modern oceanic basins. The white micas of the schists have high concentrations of the phengite end member (Table 3).

The *quartzites of the upper unit* are characterized by a fairly monotonous mineralogy. According to their quantitative variations in the proportions of rock-forming minerals, these rocks were subdivided into chlorite–epidote–amphibole, chlorite–phengite–amphibole, garnet–amphibole–mica, and mica–amphibole varieties.

GEOCHEMISTRY OF METAMORPHIC ROCKS AND THE GEODYNAMIC ENVIRONMENT IN WHICH THEY WERE PRODUCED

The chemistry and geochemistry of the metamorphic rocks of the Khavyven Formation are characterized in Table 4. The reconstructed protoliths of the deposits of the **lower unit** allowed us to distinguish its both volcanic and terrigenous protolithic material. The latter is present only locally in the upper part of the sequence and consists of micaceous and garnet–mica (±epidote, ±amphibole) quartzite-schists, whose composition corresponds to subgraywackes and, to a lesser extent, quartzites. These rocks are highly silicic and have anomalously low concentrations of alumina and alkalis [19]. Most of the porphyroblastic crystalline schists of the lower unit are metavolcanic rocks of variable silicity and compositionally correspond to andesite, dacite, rhyolite, trachyandesite, and trachydacite with the predominance of andesitic, dacitic, and trachydacitic varieties (Fig. 3a). They are characterized by elevated concentrations of Na_2O, K_2O, lithophile elements (Rb, Sr, Ba, Nb, Th, Zr, Hf, Ta, and U), and low contents of Ti, Co, Ni, Cr, and V. The rocks exhibit broad variations in the K_2O concentrations, which suggest the presence of rocks of the low-K (tholeiitic) and high-K (shoshonitic) series with the predominance of volcanics of the high-K calc–alkaline series (Fig. 3b). A notable feature of these rocks is very high Sr concentrations in some samples of the crystalline schists richest in K_2O, as was pointed out in our earlier paper [19].

[1] Mineral symbols: *Ab*—albite; *Alm*—almandine; *Bi*—biotite; *Ep*—epidote; *Gr*—garnet; *Gros*—grossular; *Hb*—amphibole; *Mu-Phn*—muscovite-phengite; *Or*—potassic feldspar; *Py*—pyrope; *Sp*—spessartine. Parts of mineral grains: *c*—core; *r*—rim. $X_{Mg} = Mg/(Mg + Fe)$.

Table 1. Representative microprobe analyses of minerals from crystalline schists of the lower unit of the Khavyven series

Component	Hv-9/3							Hv-13					
	Gr$_c$	*Gr$_r$*	*Hb$_c$*	*Hb$_r$*	*Mu-Phn*	*Ep*	*Ab*	*Gr$_c$*	*Gr$_r$*	*Hb$_c$*	*Hb$_r$*	*Bi*	*Mu-Phn*
SiO_2	37.56	37.53	49.90	47.50	52.09	39.08	69.22	37.50	37.18	47.28	43.77	37.42	50.89
TiO_2	0.00	0.00	0.01	0.12	0.06	0.03	0.00	0.19	0.05	0.25	0.20	1.66	0.37
Al_2O_3	21.54	21.40	5.24	7.90	27.48	27.26	19.20	22.19	22.22	9.55	9.97	15.75	25.33
FeO	16.52	24.38	18.15	19.00	4.05	9.28	0.02	17.07	20.66	22.08	23.30	23.41	6.87
MnO	11.56	3.91	0.05	0.06	0.00	0.33	0.00	12.05	9.84	0.28	0.33	1.46	0.00
MgO	0.38	0.65	10.96	9.80	3.06	0.12	0.00	0.19	0.24	6.06	5.88	7.60	2.44
CaO	12.60	11.89	10.53	10.40	0.00	21.65	0.00	12.53	11.39	7.90	9.81	0.14	0.00
Na_2O	0.00	0.00	1.65	1.80	0.00	0.00	10.69	0.00	0.00	4.26	2.73	0.00	0.00
K_2O	0.00	0.00	0.27	0.39	9.04	0.00	0.09	0.00	0.00	0.78	1.06	10.07	11.05
Total	100.16	99.76	96.76	96.97	95.78	97.75	99.22	101.72	101.58	98.44	97.05	96.51	96.95
X_{Mg}	0.039	0.045	0.518	0.479	0.574	0.023	–	0.019	0.020	0.328	0.310	0.366	0.388
X_{An}	–	–	–	–	–	–	0.000	–	–	–	–	–	–
Alm	36.7	54.5	–	–	–	–	–	37.4	45.3	–	–	–	–
Py	1.5	2.6	–	–	–	–	–	0.7	0.9	–	–	–	–
Sp	26.0	8.8	–	–	–	–	–	26.7	21.8	–	–	–	–
Gros	35.8	34.1	–	–	–	–	–	35.2	32.0	–	–	–	–
a_{Al}^{VI}	–	–	–	–	25.1	–	–	–	–	–	–	–	31.2
a_{Si}	–	–	–	–	13.7	–	–	–	–	–	–	–	14.5
a_K	–	–	–	–	0	–	–	–	–	–	–	–	0
Amphibole*	–	–	*Act-Hb*	*Act-Hb*	–	–	–	–	–	*Fer-Bar*	*Fer-Eden*	–	–

Component	Hv-13		Hv-75/3					1186/8					
	Ep	*Ab*	*Gr$_c$*	*Gr$_r$*	*Hb$_c$*	*Hb$_r$*	*Mu-Phn*	*Ep*	*Ab*	*Gr$_c$*	*Gr$_r$*	*Hb*	*Mu-Phn*
SiO_2	37.88	64.35	37.39	37.48	51.93	49.73	49.95	39.72	68.88	37.49	37.53	53.04	50.21
TiO_2	0.00	0.00	0.11	0.11	0.00	0.03	0.07	0.00	0.00	0.11	0.10	0.02	0.16
Al_2O_3	22.27	20.72	22.36	21.93	2.08	5.08	28.05	33.11	19.79	21.41	21.62	3.83	26.51
FeO	13.97	0.32	16.38	23.97	21.49	20.70	4.16	1.20	0.19	12.18	20.84	15.63	3.69
MnO	0.23	0.00	7.32	2.07	0.03	0.03	0.00	0.00	0.00	15.24	6.92	0.23	0.00
MgO	0.01	0.00	0.20	0.44	9.90	9.27	2.39	0.04	0.00	0.21	0.49	12.35	2.81
CaO	22.60	0.02	16.28	14.13	11.64	11.17	0.00	23.80	0.28	13.00	12.61	10.25	0.04
Na_2O	0.00	11.92	0.00	0.00	0.02	0.70	0.00	0.00	11.63	0.00	0.00	1.40	0.91
K_2O	0.00	0.09	0.00	0.00	0.13	0.34	10.69	0.00	0.05	0.00	0.00	0.05	10.47
Total	96.96	100.42	100.04	100.13	97.22	97.05	95.31	97.87	100.82	99.64	100.11	96.80	94.80
X_{Mg}	–	–	0.015	0.032	0.451	0.444	0.506	–	–	0.030	0.040	0.585	0.576
X_{An}	–	0.014	–	–	–	–	–	–	0.012	–	–	–	–
Alm	–	–	45.1	53.3	–	–	–	–	–	27.3	46.4	–	–
Py	–	–	0.7	1.7	–	–	–	–	–	0.8	2.0	–	–
Sp	–	–	14.2	4.7	–	–	–	–	–	34.6	15.6	–	–
Gros	–	–	40.0	40.3	–	–	–	–	–	37.3	36.0	–	–
a_{Al}^{VI}	–	–	–	–	–	–	23.7	–	–	–	–	–	24.9
a_{Si}	–	–	–	–	–	–	16.0	–	–	–	–	–	15.0
a_K	–	–	–	–	–	–	0	–	–	–	–	–	11.8
Amphibole*	–	–	–	–	*F-Act-Hb*	*Fer-Act*	–	–	–	–	–	*Act*	–

Table 1. (Contd.)

Component	1186/8		Hv-9/1							1185/4			
	Ep	*Ab*	Gr_c	Gr_r	Hb_c	Hb_r	*Mu-Phn*	*Ep*	*Ab*	*Bi*	*Mu-Phn*	*Ep*	*Or*
SiO_2	37.97	67.85	37.43	37.64	49.18	48.99	50.44	38.62	68.90	37.39	49.01	36.81	64.51
TiO_2	0.06	0.00	0.07	0.03	0.03	0.01	0.11	0.00	0.00	1.23	0.21	0.00	0.00
Al_2O_3	27.25	19.64	21.86	21.32	8.02	6.55	27.02	27.89	19.73	13.80	22.08	20.08	18.56
FeO	9.12	0.02	18.48	22.06	19.45	19.49	3.69	7.90	0.10	25.24	9.24	15.70	0.08
MnO	0.38	0.00	10.40	5.78	0.05	0.05	0.00	0.04	0.00	0.44	0.06	0.30	0.00
MgO	0.01	0.00	0.50	0.61	9.03	9.62	3.14	0.01	0.00	8.20	2.67	0.02	0.00
CaO	22.43	0.18	12.63	12.79	9.77	10.26	0.00	23.51	0.00	0.00	0.00	21.40	0.00
Na_2O	0.00	11.73	0.00	0.00	2.76	1.69	0.22	0.00	10.98	0.00	0.00	0.00	0.50
K_2O	0.00	0.09	0.00	0.00	0.33	0.30	11.71	0.00	0.06	9.45	8.92	0.00	15.14
Total	97.22	99.51	101.37	100.23	98.62	96.96	96.33	97.97	99.77	95.75	92.19	94.31	98.79
X_{Mg}	–	–	0.046	0.047	0.453	0.468	0.602	–	–	0.367	0.340	0.002	–
X_{An}	–	0.008	–	–	–	–	–	–	0.000	–	–	–	–
Alm	–	–	40.1	48.6	–	–	–	–	–	–	–	–	–
Py	–	–	1.9	2.4	–	–	–	–	–	–	–	–	–
Sp	–	–	22.9	12.9	–	–	–	–	–	–	–	–	–
Gros	–	–	35.1	36.1	–	–	–	–	–	–	–	–	–
a_{Al}^{VI}	–	–	–	–	–	–	25.7	–	–	–	38.9	–	–
a_{Si}	–	–	–	–	–	–	15.6	–	–	–	13.0	–	–
a_K	–	–	–	–	–	–	2.8	–	–	–	0	–	–
Amphibole*	–	–	–	–	*F-Act-Hb*	*F-Act-Hb*	–	–	–	–	–	–	–

Component	1185/4	1186/4			1182							
	Ab	*Bi*	*Mu-Phn*	*Or*	*Ab*	Gr_c	Gr_r	*Hb*	*Bi*	*Mu-Phn*	*Ep*	*Ab*
SiO_2	68.55	37.04	49.53	64.31	68.24	37.32	37.62	48.58	37.98	47.87	37.13	68.59
TiO_2	0.00	0.94	0.25	0.15	0.00	0.11	0.11	0.11	1.35	0.17	0.03	0.00
Al_2O_3	19.39	13.37	23.20	18.31	19.41	21.43	21.14	6.91	14.33	25.61	21.97	19.13
FeO	0.04	24.65	6.40	0.37	0.05	11.73	12.14	20.74	20.45	6.99	3.43	0.12
MnO	0.00	0.39	0.05	0.00	0.00	16.38	15.15	0.62	0.44	0.00	0.37	0.00
MgO	0.00	8.52	2.62	0.00	0.00	0.08	0.07	9.72	9.95	2.66	0.00	0.00
CaO	0.03	0.04	0.00	0.00	0.00	13.07	13.76	7.86	0.17	0.02	22.47	0.00
Na_2O	11.68	0.03	0.00	0.39	11.89	0.00	0.00	3.69	0.05	0.07	0.00	11.31
K_2O	0.08	9.08	9.34	15.60	0.14	0.00	0.00	0.26	9.11	10.93	0.00	0.08
Total	99.77	94.06	91.39	99.13	99.73	100.12	99.99	98.49	93.88	94.32	95.40	99.23
X_{Mg}	–	0.381	0.422	–	–	0.012	0.010	0.455	0.464	0.404	–	–
X_{An}	0.130	–	–	–	0.000	–	–	–	–	–	–	0.000
Alm	–	–	–	–	–	26.0	26.8	–	–	–	–	–
Py	–	–	–	–	–	0.3	0.3	–	–	–	–	–
Sp	–	–	–	–	–	36.7	33.8	–	–	–	–	–
Gros	–	–	–	–	–	37.0	39.0	–	–	–	–	–
a_{Al}^{VI}	–	–	31.9	–	–	–	–	–	–	23.7	–	–
a_{Si}	–	–	12.5	–	–	–	–	–	–	16.8	–	–
a_K	–	–	0	–	–	–	–	–	–	10.2	–	–
Amphibole*	–	–	–	–	–	–	–	*Bar*	–	–	–	–

Note: Samples HV-9/3, Hv-75/3, 1186/8, and Hv-9/1—garnet–epidote–amphibole–mica crystalline schists; Hv-13—garnet–epidote–amphibole–mica basic schist; 1185/4 and 1186/4—epidote–amphibole–muscovite–biotite crystalline schists; 1182—garnet–epidote–amphibole–mica quartzite. Sampling sites are at the Pravaya Kvartsevaya River.

* The amphibole nomenclature is given according to [31]: *Act*—actinolite, *Act–Hb*—actinolitic hornblende; *Fer-Act*—ferroactinolite; *F-Act-Hb*—feroactinolitic hornblende; *Fe-Bar*—ferobarroisite; *Fe-Eden*—ferroedenite. Fe^{3+} in amphiboles was calculated by the formula $Fe^{3+} = Al^{IV} - Al^{VI} - 2Ti - Na(A) - K(A) + Na(M4)$.

Mu-Phn: $a_{Al}^{VI} = (Mg + Fe + Mn + Ti)/(Mg + Fe + Mn + Ti + Al^{VI}) \cdot 100$, $a_{Si} = Al^{IV}/(Al^{IV} + Si) \cdot 100$, $a_K = Na/(Na + K)$ [32].

Table 2. Representative microprobe analyses of amphiboles from epidote–amphibole and epidote–mica–amphibole green schists of the upper unit of the Khavyven Highland

Component	1179		1187/6		1196		Hv-83/1		Hv-70		Hv-5/1
	Hb_c	Hb_r	Hb_c	Hb_r	Hb_c	Hb_r	Hb_c	Hb_r	Hb_c	Hb_r	Hb_c
SiO_2	50.62	50.50	48.18	53.03	53.76	52.20	50.23	50.10	50.84	50.02	51.40
TiO_2	0.09	0.07	0.14	0.07	0.00	0.05	0.08	0.13	0.11	0.11	0.04
Al_2O_3	5.78	5.32	7.07	3.61	2.74	4.30	6.42	6.49	5.90	6.13	4.20
FeO	15.77	15.92	20.15	16.59	14.89	17.07	18.23	18.74	17.51	16.72	17.40
MnO	0.31	0.26	0.38	0.29	0.21	0.19	0.35	0.37	0.41	0.37	0.22
MgO	12.73	12.33	9.83	13.45	14.29	12.04	10.73	10.38	11.29	11.79	12.27
CaO	7.56	8.15	7.92	10.52	11.32	8.70	6.85	6.91	7.17	7.97	8.95
Na_2O	3.26	2.80	3.44	1.48	0.98	2.70	3.56	3.56	3.30	3.41	2.42
K_2O	0.09	0.04	0.17	0.04	0.16	0.15	0.17	0.21	0.49	0.23	0.15
Total	96.21	95.39	97.28	99.08	98.35	97.40	96.62	96.89	97.02	96.75	97.05
X_{Mg}	0.585	0.576	0.460	0.597	0.631	0.557	0.508	0.497	0.535	0.557	0.557
calculated for 23											
Si	7.496	7.548	7.267	7.651	7.754	7.672	7.485	7.467	7.531	7.428	7.611
Ti	0.008	0.006	0.016	0.006	0.000	0.004	0.007	0.014	0.011	0.011	0.004
Al^{IV}	0.504	0.452	0.733	0.349	0.246	0.328	0.515	0.533	0.469	0.572	0.389
Al^{VI}	0.506	0.486	0.518	0.265	0.210	0.418	0.614	0.609	0.562	0.502	0.345
Fe^{3+}	0.631	0.525	0.608	0.399	0.235	0.365	0.629	0.621	0.568	0.487	0.473
Fe^{2+}	1.322	1.465	1.917	1.602	1.561	1.733	1.679	1.715	1.601	1.589	1.681
Mn	0.039	0.033	0.049	0.036	0.026	0.024	0.044	0.047	0.052	0.046	0.028
Mg	2.809	2.746	2.196	2.892	3.071	2.637	2.383	2.305	2.492	2.609	2.707
Ca	1.199	1.305	1.272	1.626	1.749	1.370	1.094	1.103	1.138	1.268	1.420
Na	0.936	0.812	0.999	0.414	0.274	0.769	1.028	1.029	0.948	0.981	0.695
K	0.017	0.007	0.032	0.007	0.029	0.028	0.032	0.040	0.093	0.044	0.028
Amphibole*	*Bar*	*Win*	*Bar*	*Act*	*Act*	*Act*	*Bar*	*Bar*	*Win*	*Bar*	*Act*

Component	Hv-5/1	Hv-27/1		Hv-38		Hv-83/2	Hv-85/1	1175/2	Hv-50		
	Hb_r	Hb_c	Hb_r	Hb_c	Hb_r	*Hb*	*Hb*	*Hb*	Hb_c	Hb_r	
SiO_2	51.71	49.84	51.66	52.85	51.13	49.91	50.97	49.92	51.74	52.47	
TiO_2	0.02	0.08	0.00	0.02	0.02	0.13	0.07	0.08	0.04	0.15	
Al_2O_3	3.85	6.14	4.31	3.50	4.94	7.26	6.40	6.21	5.75	2.93	
FeO	17.33	19.53	18.19	17.06	17.90	16.11	15.26	18.28	17.98	16.73	
MnO	0.26	0.16	0.11	0.24	0.27	0.09	0.23	0.46	0.24	0.32	
MgO	12.24	10.71	12.38	11.69	11.37	11.31	12.77	10.78	11.05	12.03	
CaO	9.55	8.48	9.74	9.98	9.15	7.95	8.09	8.01	9.67	10.59	
Na_2O	1.98	3.01	1.96	1.65	1.91	3.63	2.99	3.40	1.91	0.95	
K_2O	0.17	0.28	0.23	0.19	0.21	0.27	0.18	0.21	0.22	0.18	
Total	97.11	98.23	98.58	97.18	96.90	96.66	96.96	97.35	98.60	96.35	
X_{Mg}	0.557	0.494	0.548	0.550	0.531	0.556	0.599	0.512	0.523	0.562	
calculated for 23											
Si	7.633	7.384	7.445	7.781	7.589	7.383	7.466	7.423	7.540	7.789	
Ti	0.002	0.007	0.000	0.002	0.002	0.014	0.006	0.007	0.004	0.018	
Al^{IV}	0.367	0.616	0.555	0.219	0.411	0.617	0.534	0.577	0.460	0.211	
Al^{VI}	0.304	0.457	0.178	0.389	0.454	0.650	0.572	0.513	0.528	0.303	
Fe^{3+}	0.436	0.536	0.780	0.172	0.454	0.327	0.529	0.478	0.324	0.146	
Fe^{2+}	1.705	1.884	1.412	1.929	1.768	1.666	1.340	1.795	1.867	1.931	
Mn	0.033	0.020	0.014	0.030	0.034	0.012	0.028	0.058	0.030	0.040	
Mg	2.695	2.365	2.659	2.565	2.515	2.494	2.788	2.388	2.400	2.661	
Ca	1.512	1.346	1.504	1.574	1.455	1.260	1.270	1.276	1.510	1.684	
Na	0.567	0.864	0.547	0.471	0.549	1.041	0.848	0.980	0.539	0.274	
K	0.032	0.053	0.042	0.035	0.040	0.051	0.033	0.040	0.041	0.034	
Amphibole	*Act*	*Act-Hb*	*Act-Hb*	*Act*	*Act*	*Bar*	*Bar*	*Bar*	*Act*	*Act*	

Note: Samples 1179, 1187/6, 1196, Hv-83/1, Hv-70, and Hv-5/1—epidote–amphibole (±chlorite) green schists; Hv-27/1, Hv-38, Hv-83/2, and Hv-85/1—epidote–mica–amphibole green schists; 1175/2—melanocratic garnet–epidote–amphibole green schist; Hv-50—thin bed of melanocratic epidote–mica–amphibole green schist among crystalline schists of the lower unit. The amphibole nomenclature is given according to [31]: *Act*—actinolite; *Act–Hb*—actinolitic hornblende, *Bar*—barroisite; *Win*—winchite. Fe^{3+} in amphiboles was calculated by the formula $Fe^{3+} = Al^{IV} - Al^{VI} - 2Ti - Na(A) - K(A) + Na(M_4)$.

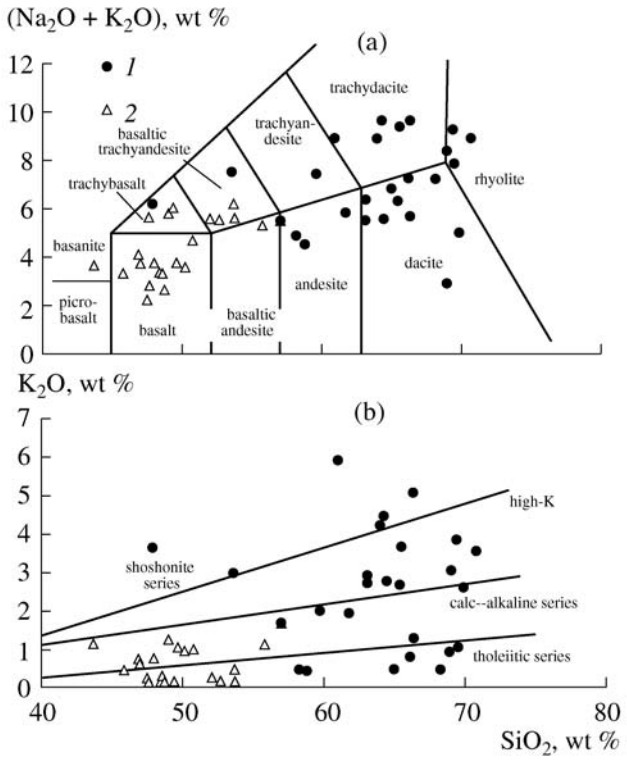

Fig. 3. Diagrams (a) ($K_2O + Na_2O$) vs. SiO_2 and (b) K_2O–SiO_2 for the metamorphic rocks of the Khavyven Highland. Based on the data of Table 4 and from [19]. Fields of volcanic series: tholeiitic, calc–alkaline, high-K calc–alkaline, and shoshonitic in the K_2O–SiO_2 diagram are given according to [33]. (*1*, *2*) Metavolcanic rocks: (*1*) lower unit of the Khavyven Formation, (b) upper unit of the Khavyven Formation.

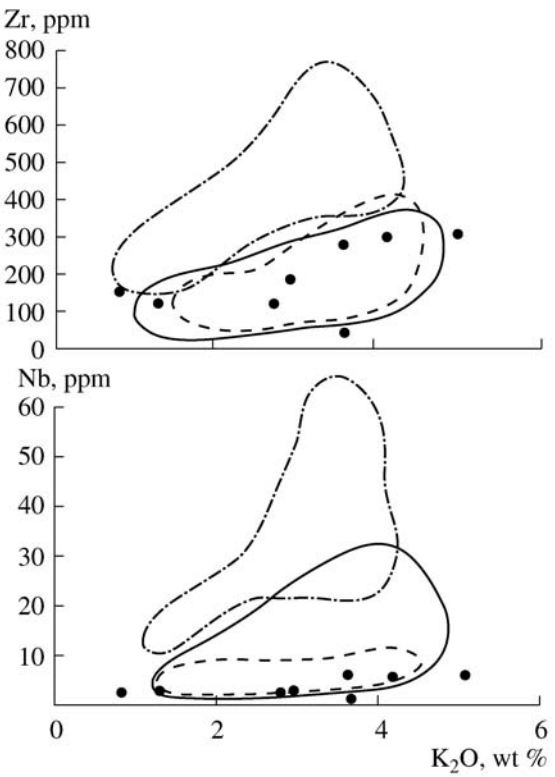

Fig. 4. Zr vs. K_2O and Nb vs. K_2O diagrams for the crystalline schists of the lower unit of the Khavyven Highland (circles). Solid line—field of island-arc lavas; dashed line—lavas of the absarokite–shoshonite–latite–trachyte series, dash–dot line—lavas of the alkaline olivine basalt series of the Sredinnyi Range of Kamchatka [34].

As can be seen in Zr–K_2O and Nb–K_2O diagrams (Fig. 4), the levels of the Nb and Zr (as well as TiO_2) concentrations in the crystalline schists are typical of island-arc volcanics, whose data points plot within the field of Late Cenozoic volcanic rocks of the high-K absarokite–shoshonite–latite–trachyte series of the Sredinnyi Range of Kamchatka. These concentrations basically differ from those in more alkaline rocks of the alkaline olivine basalt series in the same area [34]. These geochemical features of the rocks make them similar to the subalkaline volcanics of volcanic belts in continental margins [35]. They can be provisionally compared with the volcanics of the shoshonite–latite series in active continental margins [35, 36].

The first data obtained on the REE concentrations and the distribution of Sr isotopes in the metamorphic rocks of the Khavyven Formation (Table 4) make it possible to reliably explain the geochemistry of the rocks composing the upper and lower units of this formation and draw conclusions concerning the geodynamic environment in which they were formed.

The crystalline schists of the lower unit have high concentrations of LILE (K, Rb, Sr, Ba, La, Ce, Th, and U) relative to those of HFSE, as is reflected in the high Ba/Zr and La/Ta ratios in these rocks (Table 4), which are typical of the products of suprasubduction magmatism. These rocks are typically enriched in LREE and show REE patterns (Fig. 5a) similar to those of arc volcanic series. As can be seen in these diagrams, the REE patterns of the schists of the lower unit are close to those of the Campanian–Maestrichtian Kirganikskay Formation in the eastern surroundings of the Sredinnyi Range of Kamchatka [37] and the Cenozoic volcanic rocks of the high-K calc–alkaline and absarokite–shoshonite–latite–trachyte series in the northern part of this range [38]. The deep negative Eu anomalies in the REE patterns of the rocks were likely caused by the involvement of small amounts (≤1%) of subducted sediments in the magma-generating processes [39].

The multicomponent discriminant diagrams of the metavolcanics of the lower unit normalized to the primitive mantle (Fig. 5b) show deep Nb–Ta minima, as is typical of volcanics of the calc–alkaline series in suprasubductional geodynamic environments.

Geochemical data testify that the crystalline schists of the lower unit have high Ba/Nb and Th/Ta ratios, perhaps, because of the participation of fluids derived from subducted lithosphere in the magma-generating pro-

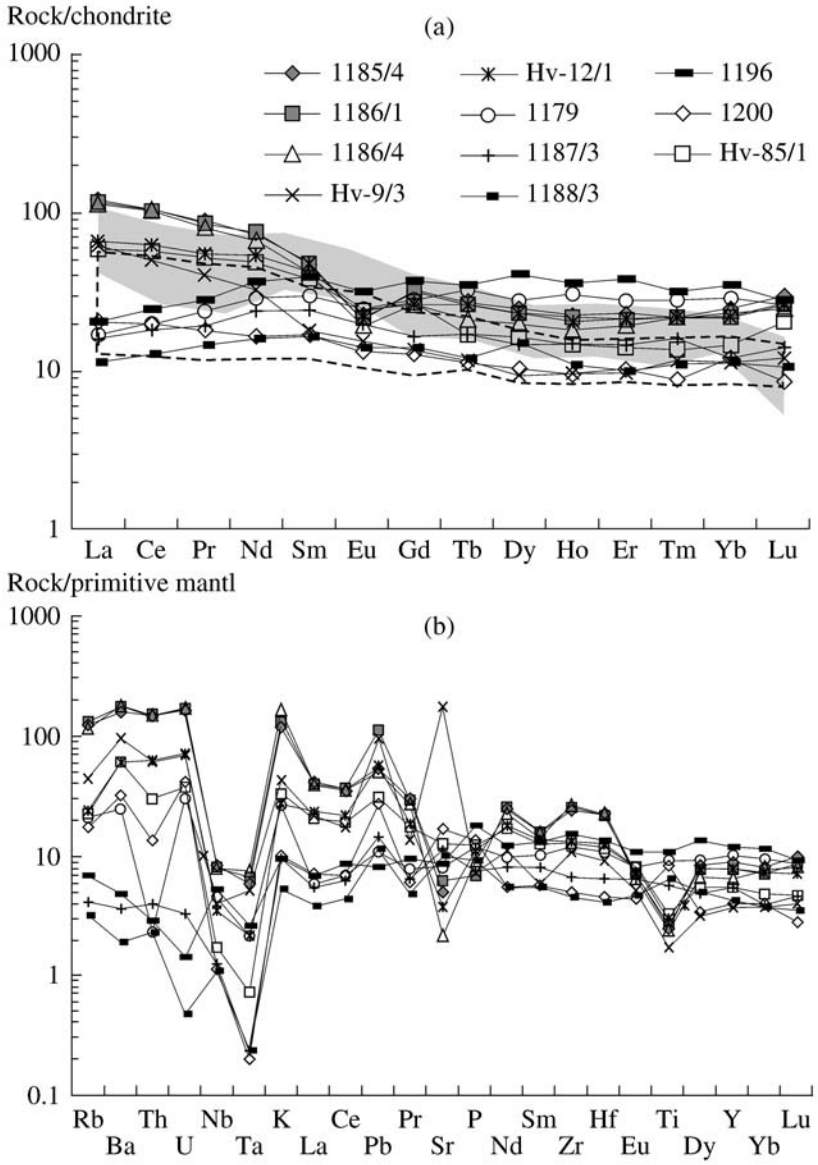

Fig. 5. (a) Chondrite-normalized [40] REE patterns and (b) multicomponent discriminant diagrams normalized to the primitive mantle [39] for the metamorphic rocks of the Khavyven Highland. Based on the data of Table 4. In Fig. 5a, dashed contour outlines the REE patterns for the Late Cretaceous–Paleogene rocks of the shoshonite series of the Kirganikskii Formation, Central Kamchatka [37]; the shaded area in the same diagram is the compositional field of the Late Cenozoic volcanic rocks of the high-K calc–alkaline and absarokite–shoshonite–latite–trachyte series of the Sredinnyi Range of Kamchatka [38].

cesses, and the high LILE concentrations relative to HFSE of the rocks, and their high $^{87}Sr/^{86}Sr$ and low Sr/Nd ratios were likely caused by the fact that the parental island-arc melts were derived from sources with small amounts of pelagic sediments that were brought to deep levels together with the subducted oceanic slab [41, 42].

The reason for the elevated $^{87}Sr/^{86}Sr$ ratio, which varies in the crystalline schists from 0.70421 to 0.70862 (Table 4), was likely the enrichment of the parental melts in a subduction phase, because the elevated Sr isotopic ratios are positively correlated with elevated concentrations of LILE. The analogous effect of the enrichment of the parental melts in the radiogenic Sr isotope can be explained by the mixing of the source of MORB tholeiites with within-plate melts. However, the low Nb contents in the rocks (Table 4) rule out the possibility of the involvement of a within-plate source with high concentrations of HFSE (Ti, Zr, Nb, and Y). Unfortunately, there are no data on the distributions of Nd and Pb isotopes in the rocks, which precludes the accurate estimation of the position of the Khavyven

Table 3. Representative microprobe analyses of micas from epidote–mica–amphibole green schists of the upper unit of the Khavyven Highland

Component	1179	Hv-5/1	Hv-29/1	Hv-38		Hv-70	Hv-83/1	Hv–83/2		Hv–85/1		1175	
	Mu-Phn	*Mu-Phn*	*Mu-Phn*	*Bi*	*Mu-Phn*	*Mu-Phn*	*Mu-Phn*	*Bi*	*Mu-Phn*	*Bi*	*Mu-Phn*	*Bi*	*Mu-Phn*
SiO_2	48.26	48.99	48.26	38.08	50.11	50.21	48.90	38.46	50.17	40.25	50.42	37.51	48.11
TiO_2	0.32	0.21	0.23	1.07	0.16	0.13	0.24	1.33	0.13	0.52	0.25	1.87	0.23
Al_2O_3	26.32	28.49	26.54	15.44	26.68	26.04	27.52	14.31	25.97	15.66	28.14	16.12	27.34
FeO	5.53	5.45	5.80	20.29	5.13	4.62	4.55	18.53	4.94	17.41	3.81	21.46	4.07
MnO	0.00	0.00	0.00	0.05	0.00	0.00	0.00	0.00	0.00	0.10	0.00	0.29	0.00
MgO	2.86	2.23	4.36	9.81	2.79	3.31	2.37	11.89	3.52	12.01	2.82	9.75	2.46
CaO	0.06	0.00	0.00	0.06	0.00	0.00	0.00	0.00	0.00	0.06	0.00	0.00	0.00
Na_2O	0.17	0.05	0.23	0.07	0.05	0.30	0.51	0.00	0.28	0.00	0.64	0.00	0.22
K_2O	10.18	10.00	10.29	9.31	10.82	10.45	10.09	10.23	10.61	9.91	10.14	9.23	10.40
Total	93.70	95.42	95.71	94.18	95.74	95.06	94.18	94.75	95.62	95.92	96.22	96.23	92.83
						calculated for 11							
Si	3.335	3.305	3.278	2.935	3.380	3.400	3.338	2.938	3.425	2.994	3.363	2.847	3.331
Ti	0.017	0.011	0.012	0.062	0.008	0.007	0.012	0.076	0.007	0.029	0.012	0.107	0.012
Al	2.146	2.268	2.127	1.400	2.123	2.080	2.217	1.290	2.092	1.374	2.214	1.443	2.234
Fe	0.320	0.308	0.329	1.308	0.289	0.262	0.260	1.184	0.282	1.082	0.212	1.362	0.236
Mn	–	–	–	0.002	–	–	–	–	–	0.004	–	0.017	–
Mg	0.295	0.224	0.441	1.127	0.280	0.334	0.241	1.354	0.235	1.331	0.280	1.103	0.254
Ca	0.005	–	–	0.006	–	–	–	–	–	0.005	–	–	–
Na	0.022	0.008	0.029	0.013	0.008	0.041	0.067	–	0.038	–	0.010	–	0.028
K	0.897	0.860	0.891	0.915	0.931	0.902	0.878	0.997	0.924	0.940	0.862	0.894	0.918
X_{Mg}	0.480	0.421	0.573	0.463	0.492	0.561	0.486	0.534	0.582	0.551	0.569	0.447	0.518
a_{Al}^{VI}	29.9	25.7	35.8	–	27.7	28.9	24.8	–	25.7	–	24.2	–	24.3
a_{Si}	16.6	17.3	18.1	–	15.5	15.0	16.6	–	14.4	–	15.9	–	16.7
a_K	2.5	0.9	3.2	–	0.9	4.3	7.0	–	4.0	–	1.1	–	3.0

Note: Sampling sites: 1179, Hv-5/1—upper reaches of the Pravaya Kvartsevaya River; Hv-29/1 and Hv-38—Ol'khovaya River; Hv-70 and 1175—Mainarka River; Hv-83/1, Hv-83/2, and Hv-85/1—Ukinskii Sevan River. $a_{Al}^{VI} = (Mg + Fe + Mn + Ti)/(Mg + Fe + Mn + Ti + Al^{VI}) \cdot 100$, $a_{Si} = Al^{IV}/(Al^{IV} + Si) \cdot 100$, $a_K = Na/(Na + K)$ [32].

Table 4. Concentrations (oxides in wt %, elements in ppm) of major and trace elements in the metamorphic rocks of the upper and lower units of the Khavyven Highland

Element	Lower unit					Upper unit					
	1185/4	1186/1	1186/4	Hv-9/3	Hv-12/1	1179	1187/3	1188/3	1196	1200	Hv-85/1
	1	2	3	4	5	6	7	8	9	10	11
SiO_2	65.55	64.01	66.31	66.34	66.11	47.93	51.98	47.62	47.44	48.51	50.74
TiO_2	0.53	0.60	0.52	0.38	0.61	2.00	1.24	1.41	2.36	1.79	0.72
Al_2O_3	15.39	14.90	15.05	16.91	15.55	13.76	16.20	15.34	13.83	14.16	17.56
Fe_2O_3	4.61	4.65	2.24	2.23	1.82	7.18	6.20	6.28	6.44	5.77	6.21
FeO	1.07	1.53	2.14	2.12	2.91	5.45	6.12	7.37	6.94	6.35	3.84
MnO	0.08	0.12	0.05	0.18	0.13	0.28	0.19	0.23	0.18	0.23	0.17
MgO	0.95	1.83	0.92	0.63	1.85	6.72	4.82	6.74	7.15	8.15	8.31
CaO	1.13	1.69	0.80	4.39	1.72	9.06	5.83	7.53	9.32	8.50	4.90
Na_2O	5.83	4.75	4.63	4.44	6.50	3.03	5.28	5.55	1.95	2.98	4.65
K_2O	3.64	4.18	5.07	1.31	0.83	0.79	0.29	0.16	0.29	0.31	1.00
P_2O_5	n.a.	0.15	0.20	0.16	0.24	0.26	0.16	0.20	0.39	0.30	0.27
H_2O^+	–	–	–	0.81	1.52	–	–	–	–	–	–
LOI	1.43	1.20	2.08	–	–	2.56	1.57	1.76	2.85	2.65	1.00
Total	100.02	99.61	100.01	99.90	99.79	99.02	99.88	100.19	99.14	99.70	99.37
V	41.00	47.47	29.32	76.45	52.97	424.19	307.09	396.09	327.96	272.33	230.55
Cr	5.32	3.30	6.35	2.83	21.47	105.45	4.53	8.17	97.14	77.16	130.80
Ni	6	8	8	20	14	70	25	26	80	57	48
Co	8.46	8.48	6.49	4.35	9.18	31.18	19.36	26.56	22.09	25.55	17.70
Cu	20.11	36.72	39.03	33.44	48.65	38.99	26.35	34.92	15.86	64.67	110.76
Zn	57.71	70.87	45.12	90.85	72.00	106.67	87.61	69.98	80.57	52.62	71.49
Ga	18.02	17.37	17.29	15.89	17.22	19.06	18.20	15.01	13.29	14.99	14.83
Ge	1.46	1.33	0.86	1.32	1.33	2.26	1.85	1.15	0.98	1.51	1.70
Rb	78.00	85.18	74.52	27.80	15.36	13.40	2.65	2.05	4.36	11.22	14.51
Sr	106.01	132.71	46.66	3695.87	78.52	169.03	235.42	215.17	184.29	363.84	270.78
Y	40.45	36.26	29.13	17.35	35.57	46.89	25.02	19.24	54.46	18.24	24.73
Zr	272.99	292.90	299.21	119.50	149.05	133.64	74.30	50.42	170.06	56.83	142.36
Nb	5.93	5.70	5.52	2.87	2.52	3.20	0.90	0.79	3.76	0.82	1.25
Sn	1.37	2.17	2.57	1.32	1.67	1.24	0.66	0.42	1.01	<0.30	0.99
Ba	1117.65	1223.33	1284.60	675.03	433.47	174.72	25.71	13.21	34.33	227.39	428.45
La	28.9	27.92	26.78	15.01	16.05	4.06	3.80	2.68	4.79	4.92	14.10
Ce	62.76	65.74	62.66	31.01	38.48	12.16	11.19	7.92	15.24	12.25	34.60
Pr	8.22	8.05	7.53	3.77	5.12	2.19	1.79	1.33	2.59	1.68	4.78
Nd	33.87	34.78	30.41	15.10	24.48	13.33	10.92	7.40	16.49	7.54	22.65
Sm	7.07	7.10	6.24	2.65	6.12	4.46	3.55	2.45	5.76	2.52	5.67

Table 4. (Contd.)

Element	Lower unit					Upper unit					
	1185/4	1186/1	1186/4	Hv-9/3	Hv-12/1	1179	1187/3	1188/3	1196	1200	Hv-85/1
	1	2	3	4	5	6	7	8	9	10	11
Eu	1.20	1.21	1.08	0.88	1.36	1.38	1.10	0.80	1.84	0.74	1.36
Gd	6.48	6.24	5.20	2.70	5.18	5.55	3.26	2.77	7.37	2.55	5.46
Tb	0.97	0.94	0.76	0.42	0.96	1.16	0.61	0.44	1.26	0.41	0.62
Dy	6.15	5.77	4.87	2.33	5.76	6.84	3.55	3.65	9.86	2.51	4.08
Ho	1.21	1.20	1.00	0.53	1.10	1.65	0.81	0.60	1.98	0.51	0.80
Er	3.75	3.34	3.10	1.56	3.51	4.49	2.29	1.59	6.01	1.67	2.25
Tm	0.53	0.53	0.54	0.29	0.54	0.70	0.39	0.27	0.79	0.22	0.34
Yb	3.99	3.55	3.70	1.85	3.52	4.71	1.93	1.84	5.62	1.95	2.36
Lu	0.73	0.64	0.61	0.30	0.52	0.64	0.35	0.26	0.69	0.21	0.35
Hf	6.94	6.70	7.06	2.81	3.95	3.39	1.98	1.27	4.14	1.42	3.64
Ta	0.24	0.27	0.31	0.21	0.09	0.09	0.01	0.01	0.11	–0.01	0.03
Pb	9.96	20.97	9.32	17.65	10.65	2.01	2.71	2.16	1.49	5.02	5.69
Th	12.75	12.82	13.00	5.14	5.37	0.20	0.34	0.20	0.25	1.14	2.59
U	3.52	3.59	3.61	1.45	1.51	0.64	0.07	0.01	0.03	0.89	0.79
$^{87}Sr/^{86}Sr \pm 2\sigma$	0.70556 ± ± 0.00021	0.70862 ± ± 0.00013	0.70764 ± ± 0.00015	0.70421 ± ± 0.00013	0.70690 ± ± 0.00008	0.70445 ± ± 0.00033	0.70480 ± ± 0.00015	0.70716 ± ± 0.00018	0.70457 ± ± 0.00020	0.70815 ± ± 0.00012	0.70704 ± ± 0.00014
K, ppm	30217.7	34700.5	42088.9	10875.0	6890.3	6558.2	2407.5	1328.3	2407.5	2573.5	8301.6
K/Rb	387.4	407.4	564.8	391.2	448.6	489.4	908.5	647.9	552.2	229.4	572.1
K/La	1045.2	1242.9	1571.7	724.5	429.3	1615.3	633.5	495.6	502.6	523.1	588.8
Na_2O/K_2O	1.60	1.14	0.91	3.39	7.83	3.84	18.21	34.69	6.72	9.61	4.65
$(La/Sm)_N$	2.55	2.46	2.68	3.54	1.64	0.57	0.67	0.68	0.5	1.22	1.55
$(La/Yb)_N$	4.92	5.34	4.92	5.51	3.11	0.59	1.34	0.99	0.58	1.71	4.06
Ba/La	38.66	43.82	47.97	44.97	27.01	43.03	6.76	4.93	7.17	46.22	30.25
Ba/Nb	188.5	214.6	232.7	235.2	172.0	54.6	28.6	16.7	9.1	277.3	341.2
Ba/Zr	4.1	4.2	4.3	5.7	2.9	1.3	0.4	0.3	0.2	4.0	3.0
Ba/Th	87.7	95.4	98.8	131.3	80.7	873.6	75.6	86.1	137.3	199.5	165.4
Th/Ta	53.1	47.5	41.9	24.5	59.7	2.2	34.0	20.0	2.3	–	86.3

Note: (1–5) Garnet ± epidote ± amphibole–mica and epidote–muscovite–biotite crystalline schists; (6–11) epidote–amphibole ± chlorite ± phengite ± biotite green schists; n.a.—not analyzed.

volcanics relative to the end members of the enriched mantle. However, the high $^{87}Sr/^{86}Sr$ ratios of these rocks testify that they belong to the trend limited by the EM2 component [43] of the enriched mantle.

By virtue of petrochemical evidence, the deposits of the **upper unit** of the Khavyven Highland were subdivided into originally volcanic and sedimentary. The sedimentary rocks are quartzites, whose composition suggests that they were formed via the metamorphism of siliceous deposits with a minor admixture of volcanic material. The metasediments also likely include thinly banded albite–magnetite–amphibole–garnet rocks, whose chemistry is comparable with that of Fe–Mn of the crusts oceanic sediments. The apovolcanic rocks compositionally correspond to albitized (spilitized) basalt (which are predominant), trachybasalts, and trachybasaltic andesites (Table 4, Fig. 3a). These rocks plot within the fields of calc–alkaline and tholeiitic series (Fig. 3b). In discriminant petrochemical diagrams [44], the green schists of the upper unit plot mostly within the fields of MORB and within-plate basalts. A distinctive compositional feature of these rocks is their high TiO_2 and Fe contents and low concentrations of K_2O and lithophile elements (Rb, Ba, and Zr), corresponding to the concentrations of these elements in normal MOR tholeiitic basalts. The metavolcanics differ from the latter in having somewhat elevated concentrations of Sr and Fe and lower concentrations of Mg, Ni, Co, and Cr, which are closer to those in volcanics from marginal basins. According to their Na_2O/K_2O ratios, the green schists are typical rocks of the K–Na subalkaline series: the Na_2O/K_2O ratios of all our samples are higher than one. The high Na/K ratio of these rocks was caused by intense spilitization of the protolithic volcanics with the replacement of their primary plagioclase by nearly pure albite.

The Ba/La and $(La/Yb)_N$ ratios of the green schists are the closest to those in MORB, although some of our samples of these rocks show slightly elevated Ba/La ratios (Table 4), which suggest a contribution of an island-arc component [45].

The chondrite-normalized REE patterns of the rocks (Fig. 5a) are depleted in LREE, $(La/Sm)_N$ = 0.5–1.5, $(La/Yb)_N$ = 0.6–4.0, analogous to the REE patterns of MOR tholeiites. The schists also show Nb/La ratios similar to those of MOR tholeiites. The multicomponent discriminant diagrams of these rocks (Fig. 5b) are similar to the diagrams of typical MORB. A significant difference is deep Nb–Ta minima in the patterns of the schists, which indicate that a subduction component was involved in the magma genesis of the protolithic volcanics [45, 46]. This conclusion finds further support in the elevated K/La (500–1600) of the rocks and their very low $(La/Yb)_N$ ratios, which range from 0.59 to 4.06 (Table 4). The contribution of the subduction component to the genesis of the green schists of the upper unit caused their high $^{87}Sr/^{86}Sr$ isotopic ratios, which vary from 0.70445 to 0.70815 (Table 4).

Our geochemical analysis of the distributions of major, trace, and rare-earth elements and Sr isotope abundances in the crystalline schists of the lower Khavyven unit testifies that their high LILE concentrations and high K/La (430–1570), Ba/Th (80–130), Th/Ta (25–60), and La/Nb (4.9–6.4) ratios (Table 4), in combination with deep Ta–Nb minima (Fig. 5) and low $(La/Yb)_N$ and high $^{87}Sr/^{86}Sr$ ratios, were predetermined by the subduction-related nature of the protolithic volcanics of the lower unit of the Khavyven Highland. This suggests that the rocks were produced in the suprasubductional environment of an ancient island arc.

The geochemistry of trace elements and REE and Sr isotopes in the metavolcanics of the upper unit of the Khavyven Formation exhibit combinations of signatures typical of depleted melts parental for MOR tholeiites and a subduction component, which caused the significant Ta–Nb minima of the rocks and their elevated K/La, low $(La/Yb)_N$, and high $^{87}Sr/^{86}Sr$ ratios. All of these data indicate that the protoliths of these rocks were formed in the environment of a marginal basin in an ancient island arc.

Thus, the geochemical data on the green schists of the upper unit indicate that the composition of these rocks shows obvious traces of the involvement of depleted sources like N-MORB and a subduction component. This confirms the conclusions [45, 46] about the heterogeneity of the magmatic sources that fed spreading processes in the marginal basins.

AGE OF METAMORPHIC ROCKS IN THE KHAVYVEN HIGHLAND

The age of the protolithic rocks of the Khavyven Highland and the age of their metamorphism are disputable. The K–Ar dates are 122, 92, and 53 Ma and are fairly uncertain and controversial [28]. $^{40}Ar/^{39}Ar$ dating on biotite from the crystalline schists of the lower unit (37.2 ± 0.4 Ma) and hornblende from the green schist of the upper unit (55 ± 5 Ma) of the Khavyven Formation point to an Early Cenozoic (Eocene) metamorphic age of the rocks [47].

We undertook an additional study of the K–Ar metamorphic age using whole-rock samples of the high-K crystalline schist of the lower unit (Table 5). The K–Ar ages are in good agreement with previously obtained $^{40}Ar/^{39}Ar$ dates and indicate that the protolithic rocks of the Khavyven Highland were metamorphosed in the Eocene in the course of Laramide tectogenesis.

DISCUSSION

The models proposed for the tectonic evolution of the Koryak–Kamchatka territory [1, 4, 14, 48–54, and others] are underlain by traditional schemes in which the territory in question is regarded as an asymmetrically zoned accretionary edifice produced under the effect of Meso-Cenozoic accretion of Pacific plates to the Asian continent. Structures in eastern Kamchatka

Table 5. K–Ar age of leucocratic epidote–mica crystalline schists of the lower unit of the Khavyven Formation

Sample	(K ± σ), wt %	($^{40}Ar_{rad}$ ± σ), ppb	K-Ar-Age, Ma
1186/1	3.53 ± 0.02	9.73 ± 0.10	39.3 ± 0.5
1186/2	3.53 ± 0.01	9.09 ± 0.27	36.8 ± 1.1
1186/4	4.50 ± 0.02	10.20 ± 0.19	32.4 ± 0.6
1185/2	3.23 ± 0.01	8.19 ± 0.53	36.2 ± 2.3

Note: The K–Ar age was determined using whole-rock samples at the Laboratory of Geochronology, Northeastern Complex Research Institute, Far East Division, Russian Academy of Sciences. The constants used in the calculations were $\lambda_k = 0.581 \times 10^{-10}$ year^{-1}; $\lambda_\beta = 4.962 \times 10^{-10}$ year^{-1}; abundance of isotopes: ^{39}Ar—93.26; ^{40}K—0.01167; ^{41}K—6.73 at %; the isotopic ratio of atmospheric Ar is $^{40}Ar/^{39}Ar = 295.5$.

include well-preserved terranes corresponding to two fossil oceanic island arcs: Ozernoi–Valaginskii (also referred to as Achaivayam–Valaginskii) and Kronotskii, which are separated by the structures of the Eastern Kamchatka Cenozoic accretionary prism [1, 10, 54]. The evolutionary histories of these structures can be traced starting in the Campanian, when the structures were supposedly formed on oceanic plates of the Northern Pacific approximately 2000–3000 km southeast of the margin of the Asian continent [1, 10, 55, 56]. Within them, extensive eruptions of lavas and tuffs of basic, intermediate, and, to a lesser extent, acid and alkaline composition were erupted. In the modern structure of eastern Kamchatka and the southern part of the Karyak Highland, the volcanic rocks of these ancient arcs compose single nappes in overthrust and imbricated structures, which were traced from Cape Goven in the north to the Valaginskii Range in the south [1].

The results of paleotectonic reconstructions suggest that the Campanian–Maestrichtian deep trench of the Ozernoi–Valaginskii island-arc system is located southwest of the active volcanic arc in the Kula plate [10]. Volcanism in this arc and its convergence with the Asian continent were caused by the rapid drift of the Kula plate relative to Eurasia. There are good reasons to believe that the modern position of the collision suture marking the fossil subduction zone of the Ozernoi–Valaginskii arc is spatially restricted to the buried Khavyven uplift of the Central Kamchatka Depression, which shows significant linear gravity anomalies [23, 24].

Active volcanism in this arc is thought to terminate in the mid-Paleocene [1, 10, 57], when the subduction zone became extinct and a new zone (dipping beneath the continent) started to form northwest of the volcanic arc. Taking into account paleomagnetic data [55, 58], the most probable timing of collision onset was the first half of the Eocene [1, 10, 59].

High-K volcanics of the calc–alkaline series are very typical of magmatic products of the Ozernoi–Valaginskii fossil island arc. These are volcanic rocks of the shoshonite–latite association [37, 60] in the Kirganikskii Formation in the eastern framing of the Sredinnyi Range of Kamchatka and alkaline ultrabasic and shoshonite–latite volcanics and their intrusive analogues in the Valaginskii and Tumrok ranges [61–64]. Melt inclusions in minerals of alkaline ultrabasic rocks of the Valaginskii Range indicate that the parental melts of these rocks were compositionally similar to the rocks of the shoshonite series [65]. Volcanic rocks of the high-K shoshonite–latite series are also characteristic of the lower unit of the Khavyven Highland, and the geochemical features of these rocks are analogous to those of the rocks of the shoshonite–latite series in central Kamchatka (Fig. 5). This suggests that the volcanics of the Khavyven Highland were also produced in the Campanian–Paleogene Ozernoi–Valaginskii fossil island arc.

In the process of accretion and tectonic thickening of the arc complexes of the Ozernoi–Valaginskii and, then, also the Kronotskii arcs and the closure of the forearc subcontinental marginal basins, the thickness of the crust in eastern Kamchatka in front of them significantly increased, and low-temperature metamorphic processes could proceed at its deep levels and form the metamorphic rocks of the Khavyven Highland. The K–Ar ages of metamorphism of the Khavyven rocks correspond to the age range of collision and accretion processes of complexes in the Ozernoi–Valaginskii and Kronotskii island arcs and the oceanic basin between them [1, 10, 59].

CONCLUSIONS

The metamorphic rocks of the Khavyven Highland were subdivided into two distinct complexes of metavolcanic rocks accompanied by subordinate amounts of metasediments. One of these complexes, which composes the lower unit of the visible vertical section of the highland, is dominated by leucocratic amphibole–mica (±garnet) and epidote–mica (±garnet) crystalline schists whose protolithic rocks were andesites and dacites and their high-K varieties of the calc–alkaline arc series. The other complex, composing the upper unit of the highland, consists of spilitized basaltoids, which were transformed into epidote–amphibole and phengite–epidote–amphibole green schists. Together with quartzites, serpentinites, and gabbroids, these schists compose a marginal-sea ophiolitic association.

The high concentrations of LILE, high K/La, Ba/Th, Th/Ta, and La/Nb ratios in combination with deep Ta–Nb minima and low $(La/Yb)_N$ and high $^{87}Sr/^{86}Sr$ ratios are demonstrated to testify to the subduction nature of the crystalline schists of the lower unit and suggest that the protolithic volcanics were generated in a suprasubduction environment of the Ozernoi–Valaginskii (Achaivayam–Valaginskii) island volcanic arc of Campanian–Paleogene age. It was determined that

the green schists of the upper unit show features typical of depleted melts like MOR tholeiites and subduction melts. This causes deep Ta–Nb minima and low $(La/Yb)_N$ and elevated K/La and $^{87}Sr/^{86}Sr$ ratios, which suggest that the green schists were formed in the environment of a marginal basin in front of the Ozernoi–Valaginskii island arc.

Newly obtained K–Ar metamorphic ages of rocks of the Khavyven Highland vary from 32.4 to 39.3 Ma and indicate that the metamorphism of the protolithic rocks took place in the Eocene and were triggered by collision and accretion processes of the island-arc complexes of the Ozernoi–Valaginskii and Kronotskii island arcs and the Asian continent and by the closure of the forearc basins in front of them. The modern position of the collision suture that marks the fossil subduction zone of the Ozernoi–Valaginskii arc is spatially restricted to the Central Kamchatka Depression and is associated with significant linear gravity anomalies.

ACKNOWLEDGMENTS

This study was financially supported by Grant no. 05-3-A-08-122 from the Far East Division of the Russian Academy of Sciences.

REFERENCES

1. *Accretionary Tectonics of Eastern Kamchatka*, Ed. by Yu. M. Pushcharovskii (Nauka, Moscow, 1993) [in Russian].
2. N. A. Bogdanov and V. D. Chekhovich, "On the Collision between the West Kamchatka and Sea of Okhotsk Plates," Geotektonika, No. 1, 72–85 (2002) [Geotectonics **36**, 63–75 (2002)].
3. V. P. Zinkevich, S. Yu. Kolodyazhnyi, L. G. Bragina, et al., "Tectonics of the Eastern Framing of the Kamchatka Sredinny Metamorphic Massif," Geotektonika, No. 1, 81–96 (1994).
4. V. P. Zinkevich and N. V. Tsukanov, "Formation of Accretionary Structures of Eastern Kamchatka in Late Mesozoic–Early Cenozoic," Geotektonika, No. 4, 97–112 (1992).
5. A. B. Kirmasov, A. V. Solov'ev, and J. K. Hourigan, "Collision and Postcollision Structural Evolution of the Andrianovka Suture, Sredinny Range, Kamchatka," Geotektonika, No. 4, 64–90 (2004) [Geotectonics **38**, 294–316 (2004)].
6. E. A. Konstantinovskaya, "The Mechanism of Continental Crust Accretion: An Example of Western Kamchatka," Geotektonika, No. 5, 59–78 (2002) [Geotectonics **36**, 393–411 (2002)].
7. A. V. Rikhter, "Structure of the Metamorphic Complex of the Sredinny Kamchatka Massif," Geotektonika, No. 1, 71–78 (1995).
8. A. V. Solov'ev, Doctoral Dissertation in Geology and Mineralogy (GIN RAN, Moscow, 2005).
9. A. V. Solov'ev, M. N. Shapiro, and J. I. Garver, "Lesnaya Nappe, Northern Kamchatka," Geotektonika, No. 6, 45–59 (2002) [Geotectonics **36**, 469–482 (2002)].
10. M. N. Shapiro, "Late Cretaceous Achaivayam–Valaginskaya Volcanic Arc, Kamchatka, and the Kinematics of North Pacific Plates," Geotektonika, No. 1, 58–70 (1995).
11. M. N. Shapiro, S. A. Solov'ev, E. A. Shcherbinina, et al., "New Data on the Time of Collision of Island Arc with Continent on Kamchatka," Geol. Geofiz. **42**, 841–851 (2001).
12. E. A. Konstantinovskaia, "Arc–Continent Collision and Subduction Reversal in the Cenozoic Evolution of the Northwest Pacific: An Example from Kamchatka (NE Russia)," Tectonophysics. **333**, 75–94 (2001).
13. *Sketches of Tectonic Evolution of Kamchatka*, Ed. by V. V. Belousov (Nauka, Moscow, 1987) [in Russian].
14. S. D. Sokolov, *Accretionary Tectonics of the Koryak–Chukot Segment of the Pacific Belt* (Nauka, Moscow, 1992) [in Russian].
15. M. N. Shapiro, P. V. Markevich, V. I. Grechin, et al., "Upper Cretaceous and Lower Paleocene Sandstones of Kamchatka: Composition and Problems of Sources," Litol. Polezn. Iskop., No. 6, 94–106 (1992).
16. A. E. Shantser, M. N. Shapiro, A. V. Koloskov, et al., "Structural Evolution of the Lesnaya Rise and Adjacent Territories in Cenozoic, North Kamchatka," Tikhookean. Geol., No. 4, 66–74 (1985).
17. A. V. Solov'ev, M. T. Brendon, J. I. Garver, et al., "Collision of the Olyutor Island Arc with the Eurasian Continental Margin: Kinematic and Age Aspects," Dokl. Akad. Nauk **360** (5), 666–668 (1998) [Dokl. Earth Sci. **361**, 632–634 (1998)].
18. Z. G. Badredinov, I. A. Tararin, A. F. Litvinov, et al., "On Nature of Metamorphic Rocks of the Khavyven Highland, Kamchatka," Dokl. Akad. Nauk SSSR **309** (2), 405–409 (1989).
19. I. A. Tararin and Z. G. Badredinov, "On the Nature of the Pre-Upper Cretaceous Basement of Eastern Kamchatka," in *New Petrological Data on the Magmatic and Metamorphic Rocks of Kamchatka*, Ed. by Yu. A. Martynov (Dal'nevost. Nauch. Ts. Akad. Nauk SSSR, Vladivostok, 1989), pp. 23–47 [in Russian].
20. A. F. Litvinov, V. B. Lopatin, N. F. Krikun, et al., "Stratigraphy of the Paleogene–Neogene Deposits of the Ozernyi Peninsula, Eastern Kamchatka," Tikhookean. Geol., No. 6, 68–77 (1990).
21. V. D. Pampura and G. P. Sandimirova, *Geochemistry and Strontium Isotopic Composition in Hydrothermal Systems* (Nauka, Novosibirsk, 1991) [in Russian].
22. I. V. Chernyshev, K. N. Shatagin, and Yu. V. Gol'tsman, "High-Precision Calibration of Strontium Isotope Standards on Multicollector Mass Spectrometer," Geokhimiya, No. 12, 1280–1285 (2000) [Geochem. Int. **38**, 1175–1180 (2000)].
23. S. E. Aprelkov and O. N. Ol'shanskaya, "Tectonic Subdivision of the Central and Southern Kamchatka Based on Geological and Geophysical Data," Tikhookean. Geol., No. 1, 53–66 (1989).
24. S. E. Aprelkov, O. N. Ol'shanskaya, and G. I. Ivanova, "Tectonics of Kamchatka," Tikhookean. Geol., No. 3, 62–75 (1991).
25. S. E. Aprelkov, L. M. Smirnov, and O. N. Ol'shanskaya, "Nature of the Anomalous Gravity Zone in the Central Kamchatka Depression," in *Deep-Seated Modeling of*

Geological Structures from Gravity and Magnetic Data, Ed. by Yu. F. Malyshev (Dal'nevost. Nauch Ts. Akad. Nauk SSSR, Vladivostok, 1985), pp. 68–71 [in Russian].

26. *Geology of the Western Bering Sea*, Ed. by S. M. Til'man and S. F. Fedorov (Nauka, Moscow, 1990) [in Russian].
27. N. V. Tsukanov, *Tectonic Evolution of Near-Oceanic Zone of Kamchatka in Late Mesozoic–Early Cenozoic* (Nauka, Moscow, 1991) [in Russian].
28. A. F. Litvinov, Candidate's Dissertation in Geology and Mineralogy (VSEGEI, Leningrad, 1990).
29. I. A. Tararin, Z. G. Badredinov, and V. M. Chubarov, "Aegirine–Augite–Crossite–Albite Metasomatics of the Ophiolite Complex of the Khavyvenskaya Range, Eastern Kamchatka," Petrologiya **5**, 99–108 (1997) [Petrology **5**, 90–100 (1997)].
30. L. L. German and S. A. Mel'nikova, "Crystalline Schists of the Ozernyi Peninsula (Eastern Coast of Kamchatka)," in *Problems of Magmatism and Tectonics of Far East*, Ed. by L. M. Parfenov (Vladivostok, 1975), pp. 3–6 [in Russian].
31. B. E. Leake, "Nomenclature of Amphiboles," Can. Mineral. **16** (4), 501–520 (1978).
32. S. P. Korikovskii, "Compositional Changes in Muscovite–Phengite Micas during Metamorphism," in *Phase Equilibria and Mineral Formation*, Ed. by I. P. Ivanov (Nauka, Moscow, 1973), Vyp. 3, pp. 71–95 [in Russian].
33. A. Peccerillo and S. R. Taylor, "Geochemistry of Eocene Calc-Alkaline Volcanic Rocks from the Kastamonu Area, Northern Turkey," Contrib. Mineral. Petrol. **58** (1), 63–81 (1976).
34. O. N. Volynets, E. I. Popolitov, M. G. Patoka, et al., "Two Series of High-Alkali Lavas in the Late Cenozoic Volcanic Zone of the Sredinnyi Range, Kamchatka," Dokl. Akad. Nauk SSSR **274** (1), 1185–1188 (1984).
35. M. I. Kuz'min, *Geochemistry of the Magmatic Rocks of Phanerozoic Mobile Belts* (Nauka, Novosibirsk, 1985) [in Russian].
36. *Geochemistry of Mesozoic Latites of Transbaikalia,* Ed. by O. M. Glazunov (Nauka, Novosibirsk, 1984) [in Russian].
37. G. B. Flerov, P. I. Fedorov, and T. G. Churikova, "Geochemistry of Late Cretaceous–Paleogene Potassic Rocks of the Early Evolutionary Stage in the Kamchatka Island Arc," Petrologiya **9**, 189–208 (2001) [Petrology **9**, 161–178 (2001)].
38. O. N. Volynets, V. S. Antipin, A. B. Perepelov, et al., "Trace Elements in Late Cenozoic–Paleogene High-Potassium Volcanic Rocks of Kamchatka," in *Geochemistry of the Voclanic Rocks of Different Geodynamic Settings*, Ed. by L. V. Tauson (Nauka, Novosibirsk, 1986), pp. 149–165 [in Russian].
39. S.-S. Sun and W. F. McDonough, "Chemical and Isotopic Systematics of Oceanic Basalts: Implications for Mantle Composition and Processes," in *Magmatism in the Ocean Basins*, Ed. by A. D. Saunders and M. J. Norry, Geol. Soc. Spec. Publ. London **42**, 313–345 (1989).
40. W. F. McDonough and S.-S. Sun, "The Composition of the Earth," Chem. Geol. **120**, 223–253 (1995).
41. R. M. Ellam and C. J. Hawkesworth, "Elemental and Isotopic Variations in Subduction Related Basalts: Evidence for a Three Component Model," Contrib. Mineral. Petrol. **98**, 72–80 (1988).
42. W. M. White and J. Patchett, "Hf–Nd–Sr Isotopes and Incompatible Element Abundances in Island Arcs: Implications for Magma Origin and Crust-Mantle Evolution," Earth Planet. Sci. Lett. **67**, 167–185 (1984).
43. A. Zindler and S. Hart, "Chemical Geodynamics," Ann. Rev. Earth Planet. Sci. **14** (2), 493–571 (1986).
44. S. D. Velikoslavinskii and V. A. Glebovitskii, "A New Discriminant Diagram for Classification of Island-Arc and Continental Basalts on the Basis of Petrochemical Data," Dokl. Akad. Nauk **401**, 213–216 (2005) [Dokl. Earth Sci. **401**, 308–310 (2005)].
45. P. I. Fedorov and N. I. Filatova, "Geochemistry and Petrology of Late Cretaceous and Cenozoic Basalts from Extensional Zones at the Continental Margin of Northeastern Asia," Geokhimiya, No. 2, 115–132 (1999) [Geochem. Int. **37**, 91–107 (1999)].
46. N. I. Filatova, "Magmatic Sources of Marginal Basins: Comparison of Magmatism of the Sea of Japan and Other Basins of the Western Pacific," Dokl. Akad. Nauk **389**, 88–94 (2003) [Dokl. Earth Sci. **389**, 252–257 (2003)].
47. V. P. Zinkevich, A. V. Rikhter, and M. M. Fugzan, "$^{40}Ar/^{39}Ar$ Dating of the Metamorphic Rocks of Eastern Kamchatka," Dokl. Akad. Nauk **333** (4), 477–480 (1993).
48. L. P. Zonenshain, M. I. Kuz'min, and L. M. Natapov, *Tectonics of Lithospheric Plates in the Territory of the USSR* (Nauka, Moscow, 1990) [in Russian].
49. E. N. Melankholina, *Tectonics of the Northwest Pacific: Relations of Oceanic and Continental Margin Structures* (Nauka, Moscow, 1988) [in Russian].
50. L. M. Parfenov, L. M. Natapov, S. D. Sokolov, et al., "Terranes and Accretionary Tectonics of Northeast Asia," Geotektonika, No. 1, 68–78 (1993).
51. *1 : 2 500 000 Tectonic Map of the Sea of Okhotsk with Explanatory Notes*, Ed. by N. A. Bogdanov and V. E. Khain (IL RAN, Moscow, 2000) [in Russian].
52. E. A. Konstantinovskaya, "The Late Cretaceous Marginal Sea of Kamchatka Peninsula," Litol. Polezn. Iskop., No. 1, 58–73 (1997) [Lithol. Miner. Resour. **32**, 50–64 (1997)].
53. E. A. Konstantinovskaya, *Tectonics of the Eastern Asian Margin: Structural Evolution and Geodynamic Modeling* (Nauchnyi Mir, Moscow, 2003) [in Russian].
54. A. V. Solov'ev, M. N. Shapiro, J. I. Garver, et al., Formation of the East Kamchatkan Accretionary Prism Based on Fission-Track Dating of Zircons from Terrigenous Rocks," Geol. Geofiz. **45** (11), 1292–1302 (2004).
55. N. A. Levashova, Candidate's Dissertation in Geology and Mineralogy (GIN RAN, Moscow, 1999).
56. N. A. Levashova and M. N. Shapiro, "Paleomagnetism of the Upper Cretaceous Island-Arc Complexes of the Kamchatka Sredinnyi Range," Tikhookean. Geol. **18** (2), 65–75 (1999).
57. M. K. Bakhteev, V. N. Ben'yamovskii, N. Yu. Bragin, et al., "New Data on Mesozoic–Cenozoic Stratigraphy of Eastern Kamchatka, Valaginskii Range," Stratigr. Geol. Korrelyatsiya **2**, 77–84 (1994).
58. D. V. Kovalenko, *Paleomagnetism of the Geological Complexes of Kamchatka and Southern Koryak Highland. Tectonic and Geophysical Interpretation* (Nauchnyi Mir, Moscow, 2003) [in Russian].

59. A. V. Solov'ev and M. N. Shapiro, "Tectonic Evolution of the Eastern Kamchatka Accretionary Prism: Evidence from Fission-Track Dating on Zircon from Terrigenous Rocks," in *Proceedings of the 38th Tectonic Conference. Tectonics of the Earth' Crust and Mantle. Tectonic Control on the Distribution of Minerals, Moscow, Russia, 2005*, Ed. by Yu. V. Koryakin (GEOS, Moscow, 2005), Vol. 2, pp. 224–228 [in Russian].

60. G. B. Flerov and A. V. Koloskov, *Alkaline Basaltic Volcanism in Central Kamchatka* (Nauka, Moscow, 1976) [in Russian].

61. V. A. Seliverstov, "Ophiolites of Eastern Kamchatka," in *Petrographic Study of Island Arc Basic Rocks*, Ed. by T. I. Frolova and V. A. Ermakov (IFZ AN SSSR, Moscow, 1978), pp. 177–239 [in Russian].

62. V. A. Seliverstov, A. V. Koloskov, and V. M. Chubarov, "Lamproite-Like Potassium Alkaline Ultramafic Rocks of the Valaginskii Range, Eastern Kamchatka," Petrologiya **2**, 197–213 (1994).

63. B. A. Markovskii and V. K. Rotman, "Geosynclinal Meymechite from Kamchatka," Dokl. Akad. Nauk SSSR **196** (3), 675–678 (1971).

64. I. N. Govorov, Z. G. Badredinov, L. N. Dardykina, et al., "Ultramafic Volcanic Rocks of the Shoshonite–Latite Series," Dokl. Akad. Nauk SSSR **310** (2), 427–431 (1990).

65. A. V. Sobolev, V. S. Kamenetskii, and N. N. Kononkova, "New Data on the Petrology and Geochemistry of Ultramafic Volcanic Rocks of the Valaginskyi Range, Eastern Kamchatka," Geokhimiya, No. 1, 1694–1709 (1989).